

Available online at www.sciencedirect.com

Physics Letters A ••• (••••) •••••

PHYSICS LETTERS A

www.elsevier.com/locate/pla

Stochastic resonance in a bistable system with time-delayed feedback and non-Gaussian noise

Dan Wu, Shiqun Zhu *

School of Physical Science and Technology, Suzhou University, Suzhou, Jiangsu 215006, People's Republic of China

Received 9 June 2006; received in revised form 27 October 2006; accepted 6 November 2006

Communicated by A.R. Bishop

Abstract

The phenomenon of stochastic resonance in a bistable system with time-delayed feedback driven by non-Gaussian noise is investigated. Combining the small time delay approximation, the path-integral approach and the unified colored noise approximation, a general approximate Fokker–Planck equation of a stochastic system is obtained. The effects of the parameter q indicating the departure from the Gaussian noise, the delay time τ , and the correlation time τ_0 of the non-Gaussian noise on the quasi-steady-state probability distribution function (SPD) and the signal-to-noise ratio (SNR) are discussed. It is found that the number of peaks in SPD and the reentrant transition between one peak and two peaks and then to one peak again in the curve of SNR depends on the parameter q , the delay time τ , and the noise correlation time τ_0 .

© 2006 Elsevier B.V. All rights reserved.

PACS: 05.60.Cd; 05.40.-a; 05.45.-a

1. Introduction

Recently, stochastic systems with time-delayed feedback have attracted much attention in various fields, such as stochastic resonance with delayed interactions [1–4], synchronized and coordinated movements with time delay [5–7], laser systems with optical feedback [8–15], feedback-regulated voltage-controlled oscillations [16–19], etc. In these systems, the time delay arises mainly due to a finite transmission speed of matter, energy, information and so on.

In last decades, stochastic resonance (SR) has been investigated extensively due to its potential applications [20–45]. Generally, SR is characterized by the optimization of the output signal-to-noise ratio (SNR) in nonlinear dynamical systems when a weak external signal is added. However, most studies of stochastic resonance neglect possible effects caused by time delays. This is mainly due to the difficulty in analytic methods of treating the non-Markovian nature of the delayed stochastic

systems [46–51]. Moreover, in most of the previous analyses about stochastic resonance, the fluctuations are assumed to be Gaussian noise sources. However, some recent experimental and theoretical results for one kind of crayfish and for rat skin offered strong indications, that there could be non-Gaussian noise sources in these sensory systems [52–58]. Thus, stochastic systems with the time-delayed feedback and non-Gaussian noise need to be investigated.

In this Letter, the phenomenon of stochastic resonance in a bistable system with time-delayed feedback driven by non-Gaussian noise is investigated. The parameter q indicating the departure from the Gaussian noise is employed to analyze the non-Gaussian noise with q -dependent probability distribution. In Section 2, methods of the small time delay approximation, the path-integral approach and the unified colored noise approximation (UCNA) are applied to obtain the approximate Fokker–Planck equation. In Sections 3 and 4, the analytic expressions of quasi-steady-state probability distribution function (SPD) and the signal-to-noise ratio of a bistable system is derived. The effects of the parameter q , the delay time τ , and the correlation time τ_0 of the non-Gaussian noise on the SPD and SNR are discussed. In Section 5, the numerical simulation is

* Corresponding author.

E-mail addresses: ys020817@suda.edu.cn (D. Wu), szhu@suda.edu.cn (S. Zhu).

employed to check the validity of the approximation methods. In Section 6, the reentrant transition between one peak and two peaks and then to one peak again in the curve of SNR is presented on the parameter planes of $(\tau-q)$, (τ_0-q) , and $(\tau-\tau_0)$. A discussion concludes the Letter.

2. General form of Fokker–Planck equation

A nonlinear dynamical system that contains time delayed feedback and non-Gaussian noise describes a non-Markov stochastic process. It is necessary to develop some approximate methods to reduce the non-Markov process to the Markov process in order to obtain analytic results. The methods of the small time delay approximation, the path-integral approach and the unified colored noise approximation can be used in the analysis [34,46–61].

A general delayed stochastic system can be described by the following differential equation

$$\frac{dx(t)}{dt} = h(x(t), x(t-\tau)) + g_1(x(t))\eta(t) + g_2(x(t))\xi(t), \quad (1)$$

where τ is the delay time of the system. The noise term $\eta(t)$ has a non-Gaussian distribution [52,53] with

$$\frac{d\eta(t)}{dt} = -\frac{1}{\tau_0} \frac{d}{d\eta} V_q(\eta) + \frac{1}{\tau_0} \varepsilon(t), \quad (2)$$

and

$$V_q(\eta) = \frac{P}{\tau_0(q-1)} \ln \left[1 + \frac{\tau_0}{P} (q-1) \frac{\eta^2}{2} \right]. \quad (3)$$

The variables $\varepsilon(t)$ and $\xi(t)$ are Gaussian white noise terms. The statistical properties of the noise terms are characterized by their first and second moments

$$\begin{aligned} \langle \varepsilon(t) \rangle &= \langle \xi(t) \rangle = 0, \\ \langle \varepsilon(t)\varepsilon(t') \rangle &= 2P\delta(t-t'), \\ \langle \xi(t)\xi(t') \rangle &= 2Q\delta(t-t'), \\ \langle \xi(t)\varepsilon(t') \rangle &= 0. \end{aligned} \quad (4)$$

Here, P and Q are the intensities of Gaussian noise terms of $\varepsilon(t)$ and $\xi(t)$. The parameter q in Eq. (3) denotes the departure from the Gaussian noise. In the limit of $q \rightarrow 1$, the process $\eta(t)$ coincides with the Gaussian colored noise with noise correlation time τ_0 . That is, it is an Ornstein–Uhlenbeck process with correlation function given by $\langle \eta(t)\eta(t') \rangle = (P/\tau_0)e^{-|t-t'|/\tau_0}$. If $q \neq 1$, $\eta(t)$ is a non-Gaussian noise term.

The stationary probability distribution of Eq. (2) can be given by [52–58]

$$P_q^{\text{st}}(\eta) = \frac{1}{Z_q} \left[1 + \frac{\tau_0}{P} (q-1) \frac{\eta^2}{2} \right]^{-1/(q-1)}, \quad (5)$$

where Z_q is a normalization constant. This distribution can be normalized only for $q < 3$ and the first and second moments of η

$$\begin{aligned} \langle \eta \rangle &= 0, \\ \langle \eta^2 \rangle &= \frac{2P}{\tau_0(5-3q)}, \end{aligned} \quad (6)$$

are finite only for $q < 5/3$.

Applying the path integral approach [56–58], one has

$$\begin{aligned} \frac{1}{\tau_0} \frac{d}{d\eta} V_q(\eta) &= \frac{\eta}{\tau_0} \left[1 + \frac{\tau_0}{P} (q-1) \frac{\eta^2}{2} \right]^{-1} \\ &\approx \frac{\eta}{\tau_0} \left[1 + \frac{\tau_0}{P} (q-1) \frac{\langle \eta^2 \rangle}{2} \right]^{-1} \\ &= \frac{\eta}{\tau_1}, \end{aligned} \quad (7)$$

with the effective noise correlation time

$$\tau_1 = \frac{2(2-q)}{5-3q} \tau_0. \quad (8)$$

In principle, the approximation applied in Eqs. (7) and (8) is only valid for $|q-1| \ll 1$.

It is clear that Eq. (2) can be reduced to a re-normalized Ornstein–Uhlenbeck process with the effective noise correlation time τ_1 and the associated effective noise intensity

$$P_1 = [2(2-q)/(5-3q)]^2 P. \quad (9)$$

From Eqs. (8) and (9), it is obvious that $\tau_1 \rightarrow \tau_0$ and $P_1 \rightarrow P$ when $q \rightarrow 1$.

So Eq. (2) of the non-Gaussian noise η can be written as

$$\frac{d\eta}{dt} = -\frac{1}{\tau_1} \eta + \frac{1}{\tau_1} \varepsilon_1(t) \quad (10)$$

and

$$\langle \varepsilon_1(t)\varepsilon_1(t') \rangle = 2P_1\delta(t-t'). \quad (11)$$

In Eqs. (2) and (3), the expression of the non-Gaussian noise [52,53] is based on the generalized thermostatics [54,55]. This kind of non-Gaussian noise has been successfully applied to a lot of physical systems [56–58]. There are also other kinds of non-Gaussian noise [52,53] that are different from Eqs. (2) and (3). However, the non-Gaussian natures of these noise terms are similar. Therefore, Eqs. (2) and (3) are chosen as a typical example of non-Gaussian noise in this Letter.

For convenience, Eq. (1) can be rewritten as

$$\frac{dx}{dt} = h(x, x_\tau) + g_1(x)\eta(t) + g_2(x)\xi(t), \quad (12)$$

where t is dropped since it is the same for all variables and x_τ denotes the time delayed state variable with $x_\tau = x(t-\tau)$.

Applying the method of UCNA [34,59–61], the non-Markov process of Eq. (12) can be written as

$$\dot{x} = \frac{1}{A(x, \tau_1)} (h(x, x_\tau) + g_1(x)\varepsilon_1(t) + g_2(x)\xi(t)) \quad (13)$$

with $A(x, \tau_1) = 1 - \tau_1 [h'(x, x) - \frac{g'_1(x)}{g_1(x)} h(x, x)]$. Here $h'(x, x)$ and $g'_1(x)$ are the derivatives of $h(x, x)$ and $g_1(x)$. It should be mentioned that the regime of the approximation method of UCNA is $A(x, \tau_1) > 0$. The method of UCNA has been justified as an adiabatic-like elimination [59,60], or as an effective Markovian Fokker–Planck approximation [61]. When applying the UCNA method to treat the colored noise in Eq. (12), it is assumed that the delay time $\tau = 0$.

Then Eq. (13) can be equivalently written as a stochastic equation

$$\frac{d}{dt}x = \tilde{h}(x, x_\tau) + \tilde{G}(x)\Gamma(t), \quad (14)$$

with

$$\begin{aligned} \langle \Gamma(t)\Gamma(t') \rangle &= 2\delta(t-t'), \\ G(x(t)) &= [P_1(g_1(x))^2 + Q(g_2(x))^2]^{1/2}, \\ \tilde{h}(x, x_\tau) &= \frac{h(x, x_\tau)}{A(x, \tau_1)}, \quad \tilde{G}(x) = \frac{G(x)}{A(x, \tau_1)}. \end{aligned} \quad (15)$$

Since the non-Gaussian colored noise term has been approximated and simplified, the effect of the time delay τ in the system can be considered to obtain approximate analytic result. Using the small time delay approximation [46–49], the delayed differential equation can be approximated as

$$\frac{dx}{dt} = h_a(x) + G_a(x)\Gamma(t) \quad (16)$$

with

$$\begin{aligned} h_a(x) &= \tilde{h}(x, x)C(x, \tau), \\ G_a(x) &= \tilde{G}(x)C(x, \tau), \\ C(x, \tau) &= 1 - \tau \frac{\partial}{\partial x_\tau} \tilde{h}(x, x_\tau) \Big|_{x_\tau=x}. \end{aligned} \quad (17)$$

Thus, the Fokker–Planck equation corresponding to Eq. (1) can be approximately written as

$$\frac{\partial P(x, t)}{\partial t} = -\frac{\partial}{\partial x}[F(x)P(x, t)] + \frac{\partial^2}{\partial x^2}[D(x)P(x, t)], \quad (18)$$

where the drift and diffusion coefficients are

$$\begin{aligned} F(x) &= h_a(x) + G_a(x) \frac{dG_a(x)}{dx}, \\ D(x) &= G_a^2(x). \end{aligned} \quad (19)$$

So the steady-state probability distribution can be analytically expressed as

$$\begin{aligned} P_{\text{st}}(x) &= \frac{N}{D(x)} \exp \left\{ \int^x dx' \frac{F(x')}{D(x')} \right\} \\ &= \frac{N}{G_a(x)} \exp \left\{ \int^x dx' \frac{h_a(x')}{G_a^2(x')} \right\}. \end{aligned} \quad (20)$$

3. Stationary probability distribution of a bistable system

When a weak periodic signal is added to a bistable system with time delay τ , the stochastic delayed differential equation follows

$$\begin{aligned} \frac{d}{dt}x(t) &= a_0x(t) - b_0x(t-\tau)^3 + x(t)\eta(t) \\ &\quad + \xi(t) + \varepsilon_0 \cos \omega t. \end{aligned} \quad (21)$$

Here $\eta(t)$ and $\xi(t)$ are the same as that in Eq. (1), $h(x, x_\tau) = a_0x - b_0x_\tau^3 + \varepsilon_0 \cos \omega t$, a_0 and b_0 are two constants of the linear and cubic terms, ε_0 is the amplitude of the signal.

It is seen that the deterministic part of Eq. (21)

$$\frac{d}{dt}x(t) = a_0x(t) - b_0x(t-\tau)^3 \quad (22)$$

is a prototypical double well potential when $\tau = 0$. When the time delay $\tau > 0$, Eq. (22) can be numerically calculated. The deterministic bifurcation diagram and the trajectory of a particle moving in the potential well are plotted in Fig. 1 when τ is varied. In Fig. 1(a), the deterministic bifurcation diagram of the maximum value x_{max} and the minimum value x_{min} of the system is plotted as a function of τ . It is seen that the particle relaxes at two stable equilibrium positions of $x_m = \pm 1.0$ when $\tau < 0.785$. For $0.785 < \tau < 1.523$, the particle begins to jump between the two potential wells and to sit in one of the well finally. For $1.523 < \tau < 1.725$, the particle moves between the two wells and finally sits on the wall of the potential well at $|x| > |x_m| = 1.0$. When $\tau > 1.725$, the particle escapes from the potential wells and the effect of bistable potential disappears. The trajectory of a particle moving in the potential well is plotted in Figs. 1(b) to (d) when τ is varied. When $\tau = 0$ in Figs. 1(b), the particle can sit in the well of $x = -1.0$ (or $x = +1.0$) if it is initially at $x < 0$ (or $x > 0$). When $\tau = 0.7$ in Fig. 1(c), the particle can move along the curve of $x < 0$ (or $x > 0$) and finally sit in the well of $x = -1.0$ (or $x = +1.0$) if it is initially at $x < 0$ (or $x > 0$). When $\tau = 1.5$ in Fig. 1(d), the particle can move along the curves cross the barrier of $x = 0$ and finally sit in either of the well of $x = -1.0$ or $x = +1.0$ no matter of its initial conditions. In the following discussions, the time delay is assumed for $\tau < 1.523$ to ensure that the system is still bistable.

From Eqs. (15) and (17), one has

$$\begin{aligned} G(x) &= (P_1x^2 + Q)^{1/2}, \\ A(x, \tau_1) &= 1 + 2b_0\tau_1x^2 + \frac{\tau_1\varepsilon_0 \cos \omega t}{x}, \\ C(x, \tau) &= 1 + \tau \frac{3b_0x^2}{1 + 2b_0\tau_1x^2}, \\ G_a(x) &= \frac{G(x)C(x, \tau)}{A(x, \tau_1)}, \\ h_a(x) &= \frac{h(x, x)C(x, \tau)}{A(x, \tau_1)}. \end{aligned} \quad (23)$$

Here, τ_1 and P_1 are the effective noise correlation time and the effective noise intensity, and are given by Eqs. (8) and (9).

Since the frequency ω is very small, there is enough time for the system to reach the local equilibrium positions during the period of $1/\omega$. Then the quasi-steady-state distribution function can be derived from Eq. (20) in the adiabatic limit

$$\begin{aligned} P_{\text{st}}(x, t) &= \frac{N}{G_a(x)} \exp \left[\frac{h(x, x)A(x, \tau_1)}{G(x)^2C(x, \tau)} \right] \\ &= \frac{N}{G_a(x)} \exp \left[-\frac{\phi(x)}{P_1} \right]. \end{aligned} \quad (24)$$

Here, N is the normalization constant, $\phi(x)$ is the rectified potential function and its form can be expressed as

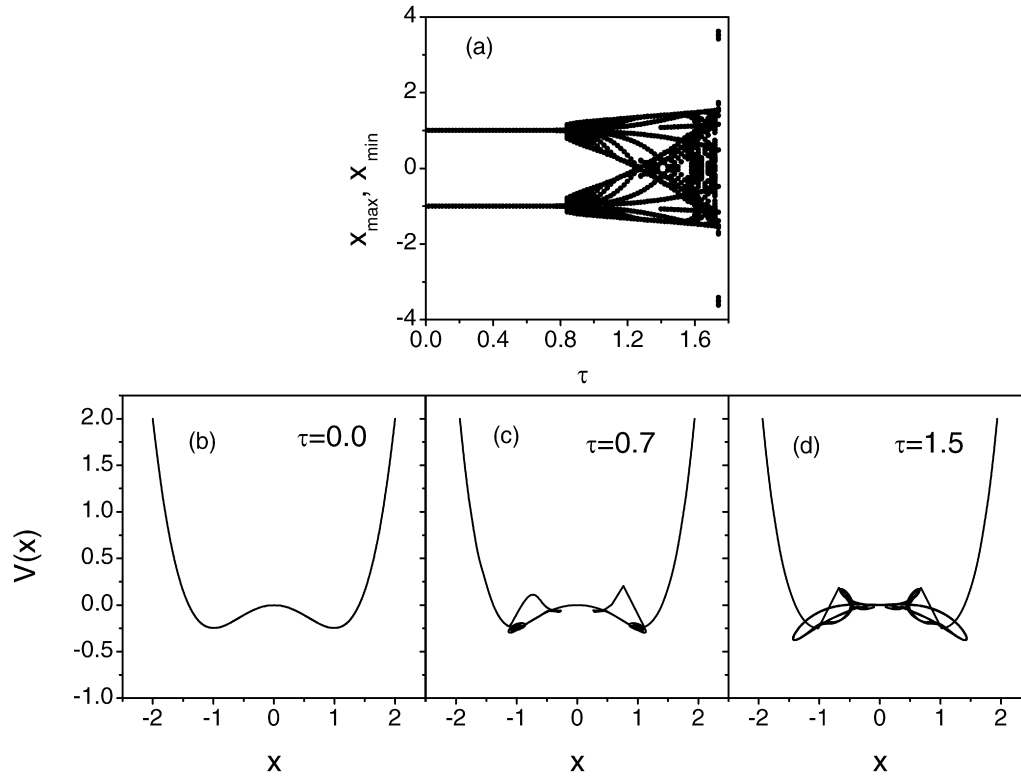


Fig. 1. The bifurcation diagram and the trajectory of a particle moving in the potential well are plotted when the time delay τ is varied. The parameters are $a_0 = 1.0$, $b_0 = 1.0$. (a) The deterministic bifurcation diagram of x_{\max} and x_{\min} is plotted as a function of τ . (b)–(d) The trajectory of a particle moving in the potential well when $\tau = 0, 0.7, 1.5$.

$$\begin{aligned} \phi(x) = & \frac{b_0^2 \tau_1^2 x^4}{2\tau_1 + 3\tau} - \alpha_1 x^2 - \alpha_2 \ln(Q + P_1 x^2) \\ & + \alpha_3 \ln[1 + b_0(2\tau_1 + 3\tau)x^2] \\ & + \left\{ -\frac{2b_0 \tau_1^2}{2\tau_1 + 3\tau} x - \beta_1 \arctan(\sqrt{P_1/Q}x) \right. \\ & \left. + \beta_2 \arctan[\sqrt{b_0(2\tau_1 + 3\tau)}x] \right\} \varepsilon_0 \cos \omega t, \end{aligned} \quad (25)$$

where

$$\begin{aligned} \alpha_1 = & \frac{2a_0 \tau_1^2}{2\tau_1 + 3\tau} - \frac{2(\tau_1 + 3\tau)}{(2\tau_1 + 3\tau)^2} + \frac{b_0 Q \tau_1}{P_1(2\tau_1 + 3\tau)}, \\ \alpha_2 = & \frac{(b_0 Q + a_0 P_1)(P_1 - 2b_0 Q \tau_1)^2}{2P_1^2 [P_1 - b_0 Q(2\tau_1 + 3\tau)]}, \\ \alpha_3 = & \frac{9P_1 \tau^2 [1 + a_0(2\tau_1 + 3\tau)]}{2(2\tau_1 + 3\tau)^3 [P_1 - b_0 Q(2\tau_1 + 3\tau)]}, \\ \beta_1 = & \frac{(P_1 - 2b_0 Q \tau_1)(P_1 - b_0 Q \tau_1 + a_0 P_1 \tau_1)}{\sqrt{Q} P_1 [P_1 - b_0 Q(2\tau_1 + 3\tau)]}, \\ \beta_2 = & \frac{3P_1 \tau (\tau_1 + 2a_0 \tau_1^2 + 3\tau + 3a_0 \tau_1 \tau)}{\sqrt{(2\tau_1 + 3\tau)^3 [P_1 - b_0 Q(2\tau_1 + 3\tau)]}}. \end{aligned} \quad (26)$$

The approximate analytical result of the steady-state probability distribution $P_{st}(x)$ (SPD) as a function of the variable x is plotted in Fig. 2 when the parameter q , the delay time τ and noise correlation time τ_0 are varied. From Fig. 2, it is clear that the curve of $P_{st}(x)$ is symmetrically located at two sides of

$x = 0$. Fig. 2(a) is a three-dimensional plot of $P_{st}(x)$ as a function of x when the parameter q is varied. The curve of $P_{st}(x)$ is changed from one peak to three peaks when q is increased. Fig. 2(d) is the contour plot of $P_{st}(x)$ on $(q-x)$ plane. There is one peak in $P_{st}(x)$ when q is in the range of $0 < q < 0.9$. When q is in the range of $0.9 < q < 1.5$, there are three peaks in $P_{st}(x)$. Fig. 2(b) is the three dimensional plot of $P_{st}(x)$ as a function of x when τ is changed. It is seen that the $P_{st}(x)$ is changed from two peaks to three peaks, and then to one peak when τ is increased. Fig. 2(e) is the contour plot of $P_{st}(x)$ on $(\tau-x)$ plane. It is seen that there are two peaks in $P_{st}(x)$ when τ is in the range of $0 < \tau < 0.7$. When τ is in the range of $0.7 < \tau < 0.9$, there are three peaks in $P_{st}(x)$. When τ is in the range of $\tau > 0.9$, there is only single peak in $P_{st}(x)$. Fig. 2(c) is the three-dimensional plot of $P_{st}(x)$ as a function of x when τ_0 is changed. It is seen that the $P_{st}(x)$ is changed from one peak to three peaks, and then to two peaks when τ_0 is increased. Fig. 2(f) is the contour plot of $P_{st}(x)$ on (τ_0-x) plane. It is seen that there is a single peak in $P_{st}(x)$ when τ is in the range of $0 < \tau_0 < 0.7$. When τ_0 is in the range of $0.7 < \tau_0 < 0.9$, there are three peaks in $P_{st}(x)$. When τ_0 is in the range of $\tau_0 > 0.9$, there are two peaks in $P_{st}(x)$.

It seems that the parameter q of the departure from the Gaussian noise can induce the transition of three peaks to one peak in $P_{st}(x)$ if q is decreased from one. The time delay τ can induce the transition of two peaks to three peaks, and then to one peak in $P_{st}(x)$ if τ is increased from zero. The noise correlation time τ_0 can induce the transition of one peak to three

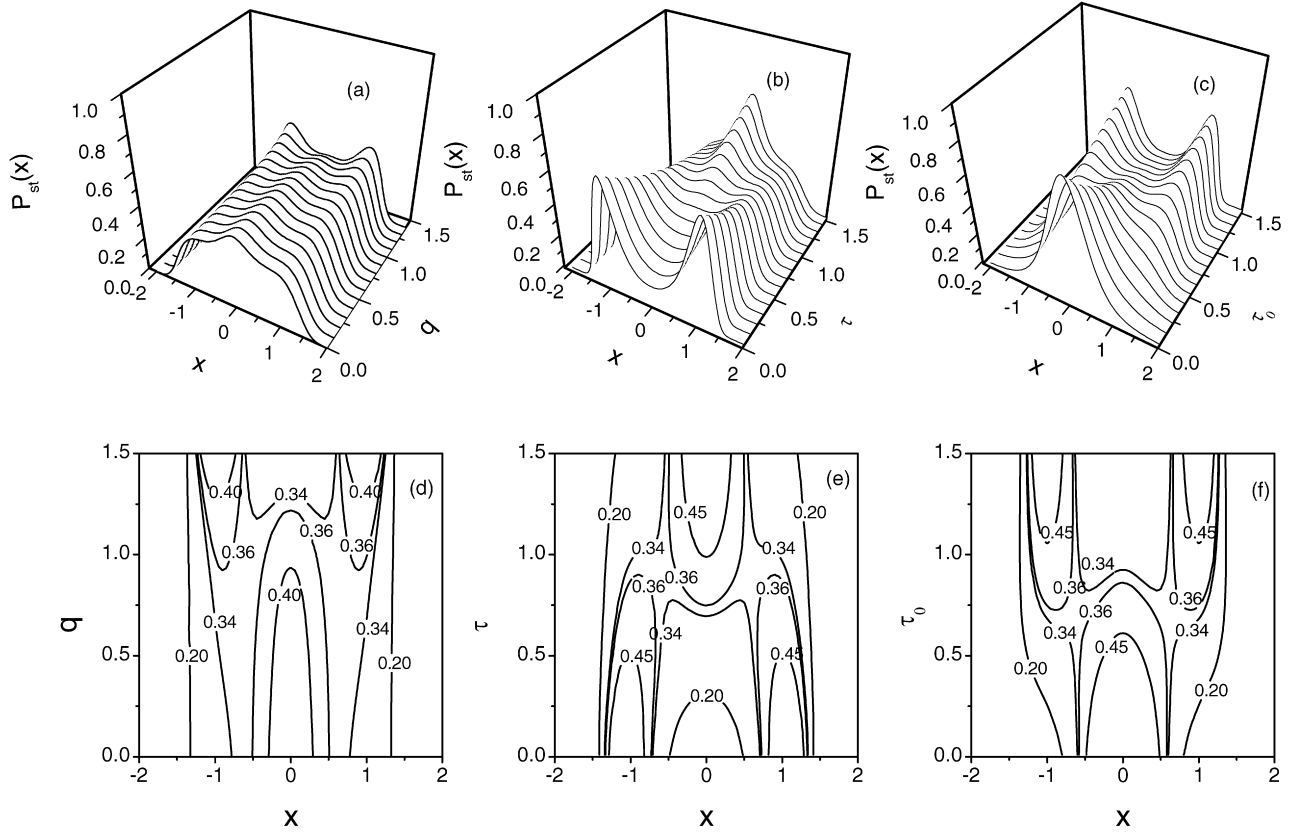


Fig. 2. The quasi-steady-state probability distribution function $P_{st}(x)$ is plotted as a function of x , the parameter q , the delay time τ and the noise correlation time τ_0 . The parameters are dimensionless and are chosen as $a_0 = 1.0$, $b_0 = 1.0$, $Q = 0.5$, $P = 0.05$, $\varepsilon_0 = 0$. (a) and (d) The $P_{st}(x)$ as a function of x when q is varied with $\tau = \tau_0 = 0.8$. (b) and (e) The $P_{st}(x)$ as a function of x when τ is varied with $\tau_0 = 0.8$, $q = 1.25$. (c) and (f) The $P_{st}(x)$ as a function of x when τ_0 is varied with $\tau = 0.8$, $q = 1.25$.

peaks, and then to two peaks if τ_0 is increased from zero. It is clear that the departure from Gaussian noise, the time delay, and the noise correlation time can modify the structure of the steady state probability distribution $P_{st}(x)$ of the system.

4. Signal-to-noise ratio

The expression of the signal-to-noise ratio (SNR) of the delayed bistable system in the adiabatic limit can be obtained from the two-state approach and can be given by [22,34,35]

$$R = \frac{\pi W_1^2 \varepsilon_0^2}{4W_0} \left[1 - \frac{W_1^2 \varepsilon_0^2}{2(W_1^2 + \omega^2)} \right]^{-1}, \quad (27)$$

where

$$W_0 = \frac{\sqrt{2}}{\pi} \exp \left[\frac{-1}{P_1} \left(-\frac{a_0^2 \tau_1^2}{2\tau_1 + 3\tau} + \frac{\alpha_1 a_0}{b_0} + \alpha_2 \ln \left[1 + \frac{a_0 P_1}{b_0 Q} \right] - \alpha_3 \ln [a_0(2\tau_1 + 3\tau) + 1] \right) \right],$$

$$W_1 = \frac{E_2}{P_1} W_0,$$

$$E_2 = \frac{2b_0 \tau_1^2}{2\tau_1 + 3\tau} + \beta_1 \arctan \left[\sqrt{\frac{a_0 P_1}{b_0 Q}} \right] - \beta_2 \arctan \left[\sqrt{a_0(2\tau_1 + 3\tau)} \right], \quad (28)$$

and $\alpha_1, \alpha_2, \alpha_3, \beta_1, \beta_2$ are given by Eq. (26). Then the SNR of the bistable system can be calculated as a function of intensity Q of noise $\xi(t)$ and intensity P of noise $\varepsilon(t)$.

From Eq. (22) and Fig. 1, it is seen that the potential of the system is a typical example of a bistable system when the time delay is $\tau < 1.523$. Therefore, the expression for the SNR derived from the two-state approach is still valid [22,34,35].

The three-dimensional plot of the SNR as a function of the intensity Q of Gaussian noise $\xi(t)$, non-Gaussian noise parameter q , delay time τ and noise correlation time τ_0 is shown in Fig. 3. Fig. 3(a) is a plot of SNR as a function of the noise intensity Q and non-Gaussian noise parameter q . Fig. 3(b) is a plot of SNR as a function of the noise intensity Q and delay time τ . Fig. 3(c) is a plot of SNR as a function of the noise intensity Q and noise correlation time τ_0 . From Figs. 3(a), (b), and (c), it is seen that the curve of SNR is changed from one peak to two peaks and then to one peak again as q , τ and τ_0 is increased respectively. The height of the major peak is increased slightly, while the height of the minor peak is increased greatly as q , τ and τ_0 are increased. Finally, the minor peak located at small value of Q becomes the major peak when the values of q , τ and τ_0 are increased further.

The three-dimensional plot of the SNR as a function of the intensity P of non-Gaussian noise $\varepsilon(t)$, non-Gaussian noise parameter q , delay time τ and noise correlation time τ_0 is shown

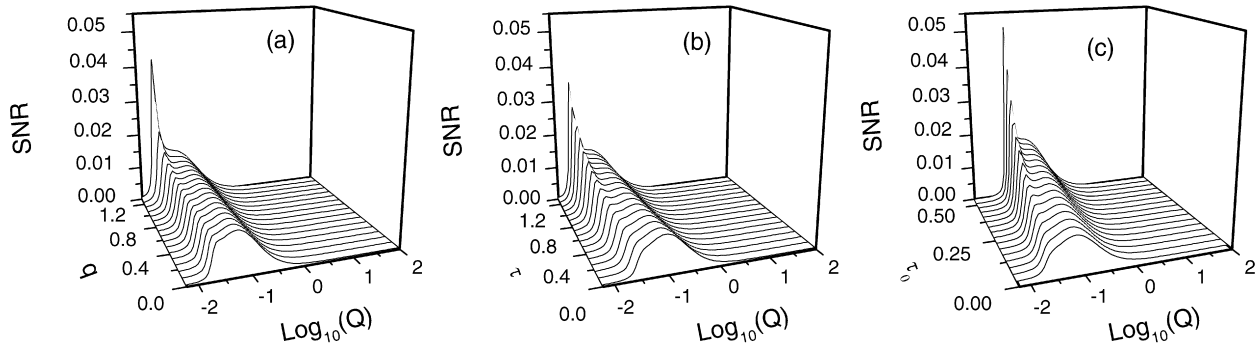


Fig. 3. Three-dimensional plot of the signal-to-noise ratio (SNR) of the delayed bistable system as a function of the intensity Q of Gaussian white noise $\xi(t)$, the parameter q , the delay time τ and the noise correlation time τ_0 . The parameters are dimensionless and are chosen as $a_0 = 1.0$, $b_0 = 1.0$, $P = 0.05$, $\omega = 0.001$, $\varepsilon_0 = 0.05$. (a) The SNR as a function of Q and q when $\tau_0 = 0.1$, $\tau = 1.0$. (b) The SNR as a function of Q and τ when $\tau_0 = 0.1$, $q = 1.25$. (c) The SNR as a function of Q and τ_0 when $\tau = 0.1$, $q = 1.25$.

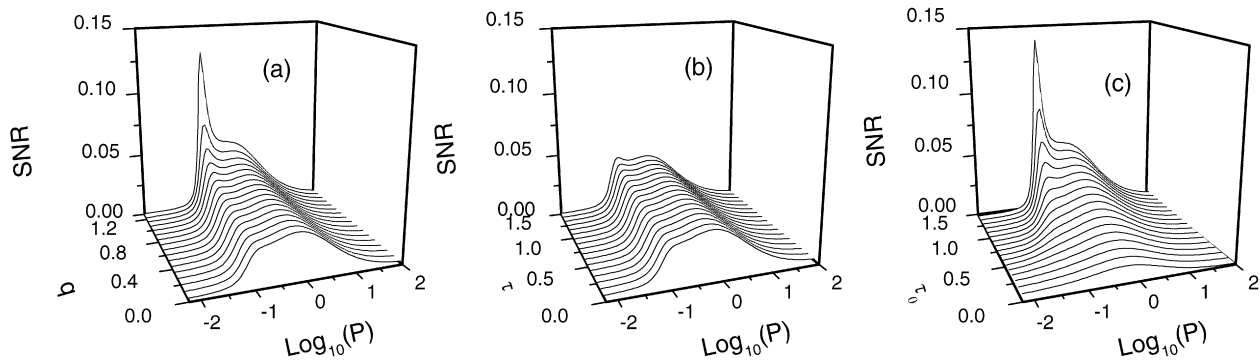


Fig. 4. The three-dimensional plot of the signal-to-noise ratio (SNR) of the delayed bistable system as a function of the intensity P of non-Gaussian noise $\eta(t)$, the parameter q , the delay time τ and the noise correlation time τ_0 . The parameters are dimensionless and are chosen as $a_0 = 1.0$, $b_0 = 1.0$, $Q = 0.05$, $\omega = 0.0023$, $\varepsilon_0 = 0.05$. (a) The SNR as a function of P and q when $\tau_0 = 0.8$, $\tau = 0.1$. (b) The SNR as a function of P and τ when $\tau_0 = 0.8$, $q = 0.65$. (c) The SNR as a function of P and τ_0 when $\tau = 0.1$, $q = 0.65$.

in Fig. 4. Fig. 4(a) is a plot of SNR as a function of the noise intensity P and non-Gaussian noise parameter q . Fig. 4(b) is a plot of SNR as a function of the noise intensity P and delay time τ . Fig. 4(c) is a plot of SNR as a function of the noise intensity P and noise correlation time τ_0 . From Figs. 4(a), (b), and (c), it is seen that the curve of SNR is changed from one peak to two peaks and then to one peak again as q , τ_0 is increased respectively. The curve of SNR is changed from one peak to two peaks as τ is increased. However, the curve of SNR is never changed to one peak again when τ is increased further. The height of the peak in SNR is increased and sharpened as q , τ , τ_0 is increased.

Compared Fig. 4 with Fig. 3, it is found that the position of the peak in SNR is located at larger value of noise intensity P .

5. Numerical simulations

In order to check the validity of the approximate methods used to obtain the analytic results, it is necessary to perform numerical simulations. The numerical simulation is performed by directly integrating the Langevin equation of Eq. (21). The numerical data of time series are obtained using the second order Runge–Kutta procedure with a time step of $\delta t = 10^{-2}$ [62, 63]. The data for each run are saved at 500 different times and 10^6 independent realizations are obtained. A histogram of 10^6

runs is constructed at 500 different times to obtain the stationary probability distribution (SPD) of $P_{st}(x)$.

The results of numerical calculations of $P_{st}(x)$ are plotted in Fig. 5 when the parameter q , the delay time τ , and the noise correlation time τ_0 are varied. Figs. 5(a), (b), and (c) are the plots of the SPD while Figs. 5(d), (e), and (f) are the plots of the parameter planes indicating the regions of one peak, two peaks, and three peaks in SPD. In Fig. 5(a), the SPD is plotted as a function of x when the parameter q is varied. From Fig. 5(a), it is seen that SPD is changed from one peak to three peaks when q is increased. Detailed comparison of Figs. 5(a) and 2(a) shows that the central peak at $x = 0$ in the numerical simulation of SPD is sharper and higher when values of q are well outside the range of $|q - 1| \ll 1$ (such as $q = 0.5$ or 1.5). In Fig. 5(b), the SPD is plotted as a function of x when the delay time τ is varied. From Fig. 5(b), it is seen that the SPD is shifted from two peaks to three peaks and then to single peak when τ is increased. Carefully comparing Figs. 5(b) with Fig. 2(b) reveals that the central peak of SPD at $x = 0$ in numerical result is sharper. In Fig. 5(c), the SPD is plotted as a function of x when the noise correlation time τ_0 is varied. From Fig. 5(c) it is seen that the SPD is shifted from single peak to three peaks and then to two peaks when τ_0 is increased. Comparison of Figs. 5(c) to Fig. 2(c) shows that the numerical results are in good agreement with the approximate solutions. From Figs. 5(b) and (c), it is

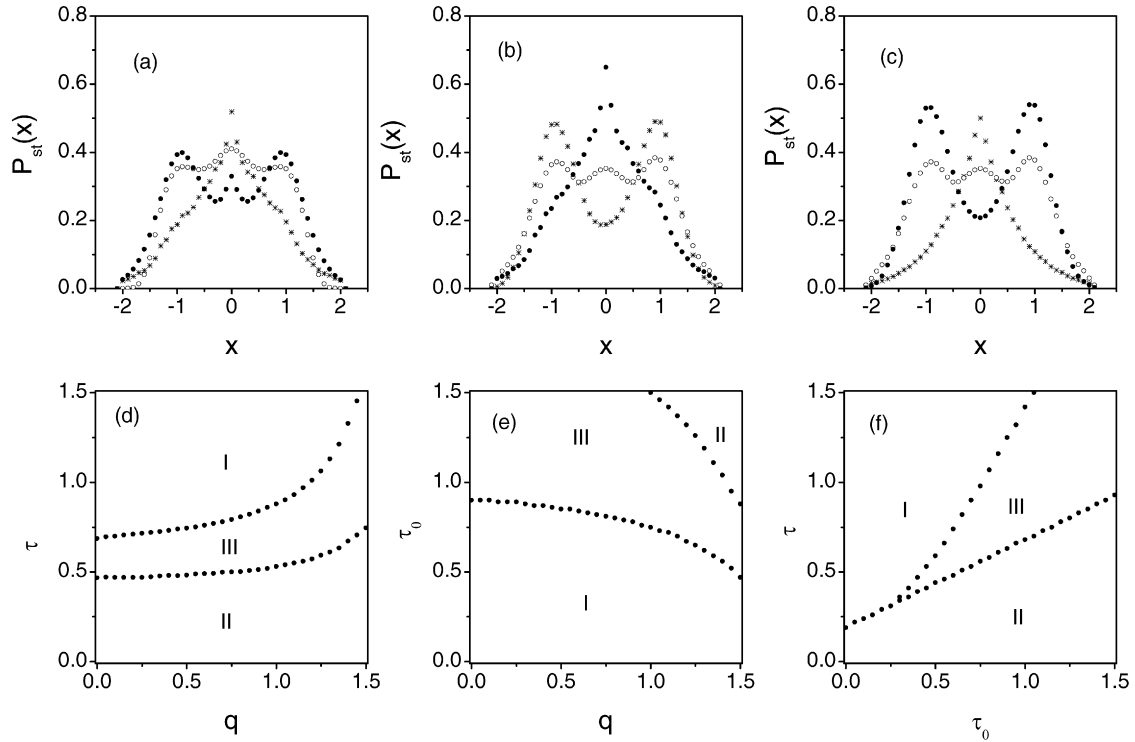


Fig. 5. The numerical simulations of $P_{st}(x)$ are plotted as a function of x when the parameter q , the delay time τ , and the noise correlation time τ_0 are varied. The parameters are dimensionless and are chosen as $a_0 = 1.0$, $b_0 = 1.0$, $Q = 0.5$, $P = 0.05$, $\varepsilon_0 = 0$. Region I means that there is a single peak in $P_{st}(x)$. Region II means that there are two peaks in $P_{st}(x)$. Region III means that there are three peaks in $P_{st}(x)$. (a) The curve of $P_{st}(x)$ as a function of x when q is changed with $\tau = \tau_0 = 0.8$ and $q = 0.5$ (*), $q = 1.0$ (o), $q = 1.5$ (•). (b) The curve of $P_{st}(x)$ as a function of x when τ is varied with $\tau_0 = 0.8$, $q = 1.25$ and $\tau = 0.4$ (*), $\tau = 0.8$ (o), $\tau = 1.5$ (•). (c) The curve of $P_{st}(x)$ as a function of x when τ_0 is varied with $\tau = 0.8$, $q = 1.25$ and $\tau_0 = 0.4$ (*), $\tau_0 = 0.8$ (o), $\tau_0 = 1.5$ (•). (d) The parameter plane of $(\tau-q)$. (e) The parameter plane of (τ_0-q) . (f) The parameter plane of $(\tau-\tau_0)$.

found that the process of the transition of the number of peaks induced by increasing τ_0 in SPD is just opposite to that induced by increasing τ . It is clear that the curves in Figs. 5(a) to (c) are in good agreement with theoretical results shown in Fig. 2.

The numerical results of the parameter planes $(\tau-q)$, (τ_0-q) , and $(\tau-\tau_0)$ are plotted in Figs. 5(d) to (f). In Figs. 5(d) to (f), it is seen that the number of peaks appeared in SPD depends on different parameter regions. Region I means that there is a single peak in $P_{st}(x)$, region II means that there are two peaks in $P_{st}(x)$, while region III means that there are three peaks in $P_{st}(x)$. From Fig. 5(d), it is clear that the SPD is changed from two peaks to three peaks and then to one peak when τ is increased and $q < 1.5$. From Fig. 5(e), it is seen that the SPD is changed from one peak to three peaks when τ_0 is increased and $q < 1.0$. When $1.0 < q < 1.5$, the SPD is changed from one peak to three peaks and then to two peaks when τ_0 is increased. From Fig. 5(f), it is seen that the SPD is changed from two peaks to one peak as τ is increased when τ_0 is in the range of $\tau_0 < 0.3$. When τ_0 is in the range of $0.3 < \tau_0 < 1.0$, the SPD is changed from two peaks to three peaks and then to single peak as τ is increased. When τ_0 is in the range of $\tau_0 > 1.0$, the SPD is changed from two peaks to three peaks as τ is increased. On the other hand, when τ satisfies $\tau < 0.185$, there are two peaks in the curve of SPD no matter how τ_0 is increased. When τ is in the range of $0.185 < \tau < 0.34$, the SPD is changed from one peak to two peaks as τ_0 is increased. When τ is in the range of $0.34 < \tau < 0.93$, the SPD is changed from one peak to three

peaks and then to two peaks as τ_0 is increased. When $\tau > 0.93$, the SPD is changed from one peak to three peaks as τ_0 is increased.

Though the time delay τ and the noise correlation time τ_0 are different and independent of each other, they are related to each other when they affect the steady state distribution $P_{st}(x)$. Except for $\tau < 0.185$, there is one kind of transition of the number of peaks in SPD when values of τ and τ_0 are small. For moderate values of τ and τ_0 , there are two kinds of transitions of the number of peaks in SPD. For large values of τ and τ_0 , there is again one kind of transition of the number of peaks in SPD.

Using the second order Runge–Kutta procedure, the numerical data of time series are calculated using a fast Fourier transform. To reduce the variance of the result, the 1024 ensembles of power spectra are averaged. The output signal-to-noise ratio is defined as $R = 10 \log_{10} S_p(\omega_s)/S_n(\omega_s)$, where $S_p(\omega_s)$ is the height of the peak in the power spectrum at the input frequency ω_s and $S_n(\omega_s)$ is the height of the noisy background in the power spectrum around ω_s .

The results of numerical calculations of the SNR are plotted in Fig. 6 when the parameter q , the delay time τ , and the noise correlation time τ_0 are varied. Figs. 6(a) to (c) are plots of the SNR as a function of the Gaussian noise intensity Q while Figs. 6(d) to (f) are plots of the SNR as a function of the non-Gaussian noise intensity P . In Figs. 6(a) and (d), the SNR is plotted when the parameter q is varied. In Figs. 6(b) and (e), the SNR is plotted when the delay time τ is varied. In

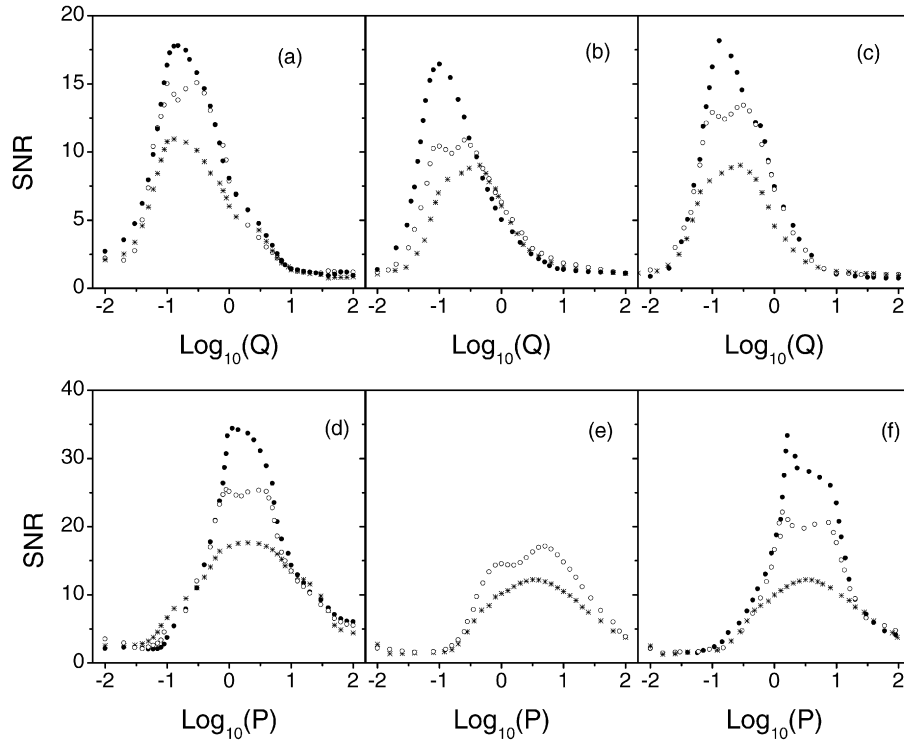


Fig. 6. Numerical simulations of the SNR are plotted as a function of the noise intensities Q and P respectively. The parameters are dimensionless and are chosen as $a_0 = 1.0$, $b_0 = 1.0$, $\varepsilon_0 = 0.05$ and $\omega = 0.001$, $P = 0.05$ in (a), (b), (c), while $\omega = 0.0023$, $Q = 0.05$ in (d), (e), (f). (a) The curve of SNR as a function of Q when q is varied with $\tau_0 = 0.1$, $\tau = 0.8$, and $q = 0.7$ (*), $q = 1.2$ (o), $q = 1.5$ (•). (b) The curve of SNR as a function of Q when τ is varied with $\tau_0 = 0.1$, $q = 1.25$, and $\tau = 0.5$ (*), $\tau = 1.2$ (o), $\tau = 1.5$ (•). (c) The curve of SNR as a function of Q when τ_0 is varied with $\tau = 0.1$, $q = 1.25$, and $\tau_0 = 0.2$ (*), $\tau_0 = 0.4$ (o), $\tau_0 = 0.6$ (•). (d) The curve of SNR as a function of P when q is varied with $\tau = 0.1$, $\tau_0 = 0.8$, and $q = 0.7$ (*), $q = 1.0$ (o), $q = 1.25$ (•). (e) The curve of SNR as a function of P when τ is varied with $\tau_0 = 0.8$, $q = 0.65$, and $\tau = 0.1$ (*), $\tau = 1.5$ (o). (f) The curve of SNR as a function of P when τ_0 is varied with $\tau = 0.1$, $q = 0.65$, and $\tau_0 = 0.8$ (*), $\tau_0 = 1.2$ (o), $\tau_0 = 1.5$ (•).

Figs. 6(c) and (f), the SNR is plotted when the noise correlation time τ_0 is varied. Compared Fig. 6 to Figs. 3 and 4, it is seen that good agreement between the theoretical results and the numerical computations is obtained.

It is clear that the approximate analytic results of the SPD and SNR plotted in Figs. 2, 3 and 4 are consistent with the computer simulations shown in Figs. 5 and 6. The agreement between the theoretical calculations and the numerical results shows that the approximation seems to work quite well for values like $q = 0.0$ and 1.5 in Figs. 2–4. That is, the approximation is still valid for values of q well outside the range of $|q - 1| \ll 1$. However, the approximation is only valid when the noise correlation time τ_0 , the delay time τ of the system, and the noise intensities P and Q are not very large. For the parameters used in this Letter, the approximation is excellent when the values of q , τ_0 , τ , P , and Q are $0.65 < q < 1.25$, $\tau_0 < 1.5$, $\tau < 1.5$, $P < 0.1$, $Q < 1.0$. When the value of q is in the range of either $0 < q < 0.65$ or $1.25 < q < 1.66$, the approximation is still valid but noticeable deviations occur in the approximate analytical results and the numerical simulations.

6. Transition of peaks in stochastic resonance

The reentrant transition between one peak and two peaks and then one peak again in stochastic resonance can be analyzed by the number of maximum peaks in the SNR of Eq. (27).

The number of the peaks in SNR as a function of the intensity Q of Gaussian noise $\xi(t)$ can be determined by the equation $\frac{dR}{dQ} = 0$ and $\frac{d^2R}{d^2Q} < 0$.

The parameter planes of $(\tau - q)$, $(\tau_0 - q)$, and $(\tau - \tau_0)$ are plotted in Fig. 7 when SNR is the maximum as a function of additive Gaussian white noise intensity Q . Areas labeled “S” mean single peak in the SNR, areas labeled “T” mean two peaks in the SNR. The areas labeled “N” mean that there is no physical meaning in these parameter regimes since SNR is less than zero in these areas. Transitions take place when non-Gaussian noise parameter q , delay time τ and noise correlation time τ_0 are varied across the boundaries of these areas.

The parameter plane of $(\tau - q)$ is plotted in Fig. 7(a) when τ_0 is fixed. From Fig. 7(a), it is seen that there is only a single peak in the SNR as τ is increased when the non-Gaussian noise parameter q is in the region of $q < 0.525$. When the parameter q is in the region of $0.525 < q < 1.134$, the SNR is changed from single peak to two peaks when τ is increased. When q is in the region of $1.134 < q < 1.5$, the SNR is changed from single peak to two peaks, and then to single peak again as τ is increased.

The parameter plane of $(\tau_0 - q)$ is plotted in Fig. 7(b) when τ is fixed. From Fig. 7(b), it is seen that the SNR is changed from single peak to two peaks, and then to single peak again as τ_0 is increased when the parameter q is in the region of $0 < q < 1.45$. The area of no physical meaning is increased as the

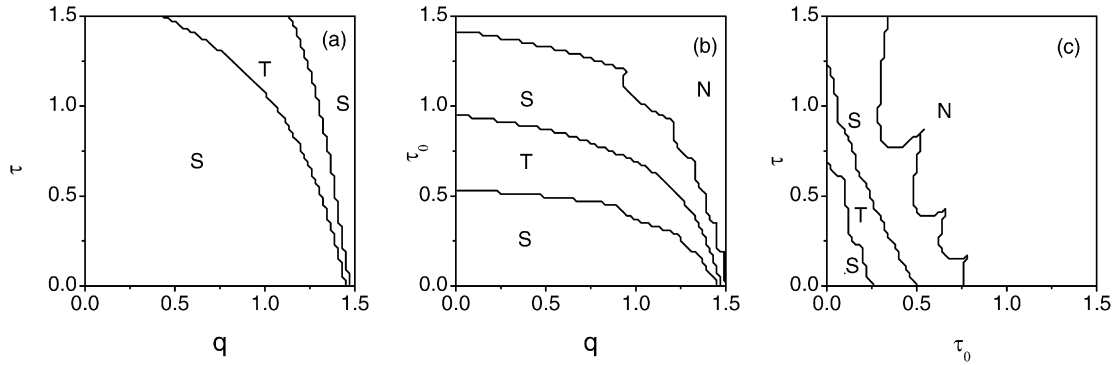


Fig. 7. The parameter planes are plotted when the curve of SNR is plotted as a function of the Gaussian white noise intensity Q . The area labeled “S” means that there is a single peak in the SNR. The area labeled “T” means that there are two peaks in SNR. The area labeled “N” means that there is no physical meaning in these parameter regimes. The parameters are dimensionless and are chosen as $a_0 = 1.0$, $b_0 = 1.0$, $P = 0.05$, $\varepsilon_0 = 0.05$, $\omega = 0.001$. (a) The parameter plane of $(\tau-q)$ with $\tau_0 = 0.1$. (b) The parameter plane of (τ_0-q) with $\tau = 0.1$. (c) The parameter of $(\tau-\tau_0)$ with $q = 1.25$.

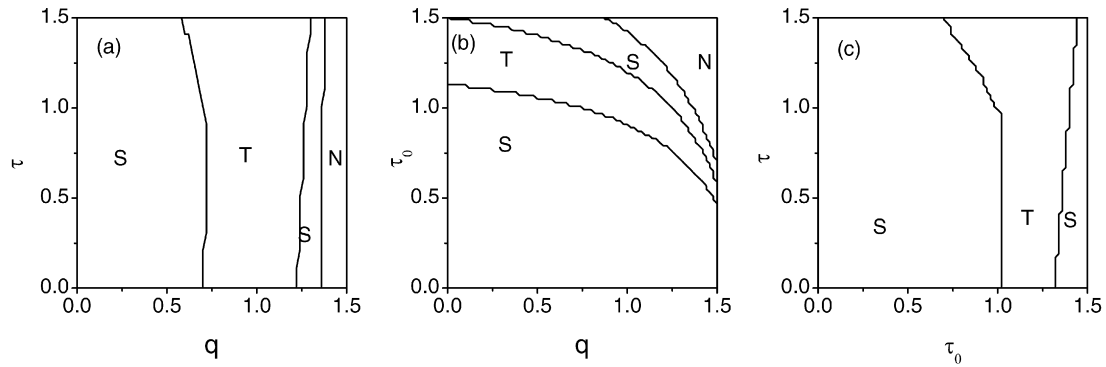


Fig. 8. The parameter planes are plotted when the curve of SNR is plotted as a function of the non-Gaussian noise intensity P . The area labeled “S” means that there is a single peak in the SNR. The area labeled “T” means that there are two peaks in SNR. The area labeled “N” means that there is no physical meaning in these parameter regimes. The parameters are dimensionless and are chosen as $a_0 = 1.0$, $b_0 = 1.0$, $Q = 0.05$, $\varepsilon_0 = 0.05$, $\omega = 0.0023$. (a) The parameter plane of $(\tau-q)$ with $\tau_0 = 0.8$. (b) The parameter plane of (τ_0-q) with $\tau = 0.1$. (c) The parameter plane of $(\tau-\tau_0)$ with $q = 0.65$.

parameter q is increased. The area of no physical meaning in Fig. 7(b) shows that the theory is only valid when the time delay τ is less than 1.42 and q is less than 1.5.

The parameter plane of $(\tau-\tau_0)$ is plotted in Fig. 7(c) when q is fixed. From Fig. 7(c), it is seen that the SNR is changed from single peak to two peaks, and then to single peak again as τ is increased when τ_0 is in the range of $0 < \tau_0 < 0.3$. When τ_0 is in the range of $0.3 < \tau_0 < 0.5$, the SNR is changed from two peaks to one peak as τ is increased. When τ_0 is in the range of $0.5 < \tau_0 < 0.75$, there is only single peak in the SNR as τ is increased. The area of no physical meaning is increased as τ_0 is increased. Meanwhile, when $\tau < 0.7$, the SNR is changed from one peak to two peaks, and then to one peak again as τ_0 is increased. When τ is in the range of $0.7 < \tau < 1.25$, the SNR is changed from two peaks to one peak as τ_0 is increased. When $\tau > 1.25$, there is only one peak in SNR as τ_0 is increased. The transition of the number of peaks in SNR may occur in the left part of the area roughly divided by the line connected $\tau = 1.5$ and $\tau_0 = 0.75$. The area of no physical meaning in Fig. 7(c) shows that the theory is only valid when the noise correlation time τ_0 is less than 0.75.

The number of peaks in SNR as a function of intensity P of the non-Gaussian noise $\varepsilon(t)$ can be determined by the equation $\frac{dR}{dP} = 0$ and $\frac{d^2R}{d^2P} < 0$.

The parameter planes of $(\tau-q)$, (τ_0-q) , and $(\tau-\tau_0)$ are plotted in Fig. 8 when SNR is the maximum as a function of the non-Gaussian noise intensity P . Areas labeled “S” mean single peak in the SNR, areas labeled “T” mean two peaks in the SNR. The areas labeled “N” mean that there is no physical meaning in these parameter regimes. Transitions take place when the non-Gaussian noise parameter q , the delay time τ and the noise correlation time τ_0 are varied across the boundaries of these areas.

The parameter plane of $(\tau-q)$ is plotted in Fig. 8(a) when τ_0 is fixed. From Fig. 8(a), it is seen that there is only a single peak in SNR no matter τ is increased or not when the parameter q is in the range of $0 < q < 0.54$. When q is in the range of $0.54 < q < 0.72$, the SNR is changed from single peak to two peaks when τ is increased. When q is in the range of $0.72 < q < 1.2$, there are two peaks in the SNR and no transition takes place in SNR as τ is changed. When q is in the range of $1.2 < q < 1.32$, there is only a single peak in SNR. When q is in the range of $q > 1.32$, it is the area of no physical meaning. That is, the theory is only valid for $q < 1.32$.

The parameter plane of (τ_0-q) is plotted in Fig. 8(b) when τ is fixed. From Fig. 8(b), it is seen that the SNR is changed from single peak to two peaks, and then to a single peak again when τ_0 is increased when the parameter q is in the range of

$0 < q < 1.5$. When q is in the range of $q > 0.86$ with $\tau_0 > 0.75$, there exists an area of no physical meaning in SNR.

The parameter plane of $(\tau-\tau_0)$ is plotted in Fig. 8(c) when q is fixed. From Fig. 8(c), it is seen that there is only single peak in SNR as τ is increased when τ_0 is in the range of $0 < \tau_0 < 0.7$. When τ_0 is in the region of $0.7 < \tau_0 < 1.05$, the SNR is changed from single peak to two peaks as τ is increased. When τ_0 is in the range of $1.05 < \tau_0 < 1.3$, there are two peaks in SNR as τ is increased. When τ_0 is in the range of $1.3 < \tau_0 < 1.4$, the SNR is changed from one peak to two peaks as τ is increased. When τ_0 is in the range of $\tau > 1.4$, there is only single peak in the SNR as τ is increased. However, no matter how the delay time τ is varied, the SNR can always be changed from single peak to two peaks and then to single peak again as τ_0 is increased.

From Figs. 7 and 8, it can be found that there always exists some areas of reentrance-like transition between one peak and two peaks in the curve of SNR when the parameter q , the delay time τ , and the noise correlation time τ_0 are varied.

7. Discussion

The phenomenon of stochastic resonance in a bistable system with time-delayed feedback driven by non-Gaussian noise is investigated. Combining the methods of the small time delay approximation, the path-integral approach and the unified colored noise approximation, a general approximate Fokker-Planck equation of the system is obtained. The quasi-steady-state probability distribution function of the system is derived. The signal-to-noise ratio is calculated in the adiabatic limit. The effects of delay time τ , correlation time τ_0 of the non-Gaussian noise, and the parameter q indicating the departure from the Gaussian noise are discussed. The critical lines are plotted on the parameter planes of $(\tau-q)$, (τ_0-q) , and $(\tau-\tau_0)$. These critical lines separate single peak, two peaks, three peaks, and nonphysical meaning areas in the curves of SPD and SNR. It is found that the reentrant transition between one peak and two peaks in the curve of SNR appears when the parameter q , the delay time τ , and the correlation time τ_0 of the non-Gaussian noise are varied. The areas of no physical meaning also provide the limitations of the parameters used in the theory.

The phenomenon of multiple peaks in the SNR has also been found for different models [22,31,43,44]. It seems that the multiple peaks in SNR can be induced by either periodic or multiple maxima and minima in the potential [31]. In this Letter, the two-peak structure appeared in SNR is mainly induced by the parameter q , the delay time τ , and the non-Gaussian noise correlation time τ_0 .

Acknowledgements

The financial support from the Natural Science Foundation of Jiangsu Province (Grant No. BK2001138) is gratefully acknowledged.

References

[1] H. Haken, Eur. Phys. J. B 18 (2000) 545.

- [2] S. Kim, S.H. Park, H.B. Pyo, Phys. Rev. Lett. 82 (1999) 1620.
 [3] T. Ohira, Y. Sato, Phys. Rev. Lett. 82 (1999) 2811.
 [4] M.K.S. Yeung, S.H. Strogatz, Phys. Rev. Lett. 82 (1999) 648.
 [5] P. Tass, J. Kurths, M.G. Rosenblum, G. Guasti, H. Hefter, Phys. Rev. E 54 (1996) R2224.
 [6] R. Engbert, C. Scheffczyk, R.T. Krampe, M. Rosenblum, J. Kurths, R. Kliegl, Phys. Rev. E 56 (1997) 5823.
 [7] Y. Chen, M. Ding, J.A.S. Kelso, Phys. Rev. Lett. 79 (1997) 4501.
 [8] F.A. Hopf, D.L. Kaplan, H.M. Gibbs, R.L. Shoemaker, Phys. Rev. A 25 (1982) 2172.
 [9] H.M. Gibbs, F.A. Hopf, D.L. Kaplan, R.L. Shoemaker, Phys. Rev. Lett. 46 (1981) 474.
 [10] F.T. Arecchi, G. Giacomelli, A. Lapucci, R. Meucci, Phys. Rev. A 45 (1992) R4225.
 [11] I. Fischer, O. Hess, W. Elsaer, E. Gobel, Phys. Rev. Lett. 73 (1994) 2188.
 [12] G. Giacomelli, R. Meucci, A. Politi, F.T. Arecchi, Phys. Rev. Lett. 73 (1994) 1099.
 [13] B. Krauskopf, G.R. Gray, D. Lenstra, Phys. Rev. E 58 (1998) 7190.
 [14] A.N. Pisarchik, R. Meucci, F.T. Arecchi, Phys. Rev. E 62 (2000) 8823.
 [15] C. Masoller, Phys. Rev. Lett. 88 (2002) 034102.
 [16] W. Wischert, A. Wunderlin, A. Pelster, M. Olivier, J. Grosblambert, Phys. Rev. E 49 (1994) 203.
 [17] C. Simmendinger, A. Wunderlin, A. Pelster, Phys. Rev. E 59 (1999) 5344.
 [18] M. Schanz, A. Pelster, Phys. Rev. E 67 (2003) 056205.
 [19] L. Langer, J.P. Goedgebuer, T. Erneux, Phys. Rev. E 69 (2004) 036210.
 [20] H. Sompolinsky, D. Golomb, D. Kleinfeld, Phys. Rev. A 43 (1991) 6990.
 [21] R. Benzi, A. Sutera, A. Vulpiani, J. Phys. A 14 (1981) L453.
 [22] B. McNamara, K. Wiesenfeld, Phys. Rev. A 39 (1989) 4854.
 [23] T. Zhou, F. Moss, Phys. Rev. A 41 (1990) 4255.
 [24] P. Jung, P. Hänggi, Phys. Rev. A 44 (1991) 8032.
 [25] G. Hu, G.R. Qing, D.C. Gong, X.D. Weng, Phys. Rev. A 44 (1991) 6414.
 [26] M.I. Dykman, R. Mannella, P.V.E. McClintock, N.G. Stocks, Phys. Rev. Lett. 68 (1992) 2985.
 [27] A. Neiman, L. Schimansky-Geier, Phys. Rev. Lett. 72 (1994) 2988.
 [28] L. Gamma, F. Marchesoni, S. Santucci, Phys. Rev. Lett. 74 (1995) 1052.
 [29] J.F. Lindner, B.K. Meadows, W.L. Ditto, M.E. Inchiosa, A.R. Bulsara, Phys. Rev. Lett. 75 (1995) 3.
 [30] A.A. Zaikin, J. Kurths, L.S. Geier, Phys. Rev. Lett. 85 (2000) 227.
 [31] J.M.G. Vilar, J.M. Rubi, Phys. Rev. Lett. 78 (1997) 2882.
 [32] J.M.G. Vilar, J.M. Rubi, Phys. Rev. Lett. 78 (1997) 2886.
 [33] J.M.G. Vilar, J.M. Rubi, Phys. Rev. Lett. 81 (1998) 14.
 [34] L. Gammaitoni, P. Hänggi, P. Jung, F. Marchesoni, Rev. Mod. Phys. 70 (1998) 223.
 [35] C. Nicolis, Tellus 34 (1982) 1.
 [36] V. Berdichevsky, M. Gitterman, Phys. Rev. E 60 (1999) 1494.
 [37] F. Marchesoni, F. Apostolico, S. Santucci, Phys. Rev. E 59 (1999) 3958.
 [38] M.M. Alibegov, Phys. Rev. E 59 (1999) 4841.
 [39] Y. Jia, S. Yu, J. Li, Phys. Rev. E 62 (2000) 1869.
 [40] H.E. Plesser, T. Geisel, Phys. Rev. E 63 (2001) 031916.
 [41] X. Luo, S. Zhu, Phys. Rev. E 67 (2003) 021104.
 [42] Q.S. Li, R. Zhu, Phys. Rev. E 64 (2001) 051116.
 [43] R. Rozenfeld, A. Neiman, L. Schimansky-Geier, Phys. Rev. E 62 (2000) R3031.
 [44] G. Mato, Phys. Rev. E 59 (1999) 3339.
 [45] J.M. Buldu, J. Garcia-Ojalvo, M.C. Torrent, Phys. Rev. E 69 (2004) 046207.
 [46] S. Guillouezic, I.L. Heuroux, A. Longtin, Phys. Rev. E 59 (1999) 3970.
 [47] S. Guillouezic, I.L. Heuroux, A. Longtin, Phys. Rev. E 61 (2000) 4906.
 [48] T.D. Frank, Phys. Rev. E 69 (2004) 061104.
 [49] T.D. Frank, Phys. Rev. E 71 (2005) 031106.
 [50] H. Hasegawa, Phys. Rev. E 70 (2004) 021911.
 [51] A.A. Budini, M.O. Caceres, Phys. Rev. E 70 (2004) 046104.
 [52] L. Borland, Phys. Lett. A 245 (1998) 67.
 [53] L. Borland, Phys. Rev. E 57 (1998) 6634.
 [54] C. Tsallis, J. Stat. Phys. 52 (1988) 479.
 [55] E.M.F. Curado, C. Tsallis, J. Phys. A 24 (1991) 3187.
 [56] M.A. Fuentes, R. Toral, H.S. Wio, Physica A 295 (2001) 114.
 [57] M.A. Fuentes, H.S. Wio, R. Toral, Physica A 303 (2002) 91.

- [58] S. Bouzat, H.S. Wio, *Physica A* 351 (2005) 69.
- [59] P. Hänggi, P. Jung, *Adv. Chem. Phys.* 89 (1995) 239.
- [60] P. Jung, P. Hänggi, *Phys. Rev. A* 35 (1987) 4464.
- [61] H.S. Wio, P. Colet, M. San Miguel, L. Pesquera, M.A. Rodriguez, *Phys. Rev. A* 40 (1989) 7312.
- [62] R.F. Fox, I.R. Gatland, R. Roy, G. Vemuri, *Phys. Rev. A* 38 (1988) 5938.
- [63] W.H. Press, S.A. Teukolsky, W.T. Vetterling, B.P. Flannery, *Numerical Recipes in FORTRAN*, second ed., Cambridge Univ. Press, Cambridge, 1992.